13th World Conference on Earthquake Engineering
Vancouver, B.C., Canada
August 1-6, 2004
Paper No. 2351

EXPERIMENTAL STUDY ON COUPLED VIBRATION CONTROL STRUCTURES

Susumu MINAMI[1], Shinji YAMAZAKI[2], Kai TOYAMA[3] and Kenichi TAHARA[4]

SUMMARY

A coupled vibration control is a method for reducing earthquake responses by connecting buildings with different periods using connecting mechanisms (dampers). In this study, shaking table tests were carried out for earthquake response of connected building models using steel hysteresis dampers to experimentally study the vibration control effects. In addition to the tests, analyses were also conducted. These tests and analyses resulted in obtaining the following conclusions. (1) The greater the difference of the natural period between two buildings, the higher the vibration control effects. (2) There is a range for the stiffness and the yield strength of a damper in which optimum vibration control can be obtained.

INTRODUCTION

A coupled vibration control is a method for reducing earthquake responses by connecting buildings with different periods using connecting mechanisms. Theoretical, analytical and experimental studies on this system have been carried out and it has been applied to some buildings. (Kobori [1], Kageyama et al. [2])

In this study, coupled vibration control structures with inelastic hysteresis dampers at the connecting parts are investigated. It is difficult to deal with structures with inelastic dampers from the theoretical point of view because of the nonlinear behavior of connecting devices. The efficiency of the coupled vibration control structures with inelastic dampers was confirmed in previous studies. However, most of the studies have been carried out only on their characteristics under limited conditions. The basic vibration control characteristics of this system have yet to be made clear. In this paper, through carrying out shaking table tests using small models the relationship between the characteristics of dampers and the vibration control effects is experimentally investigated. Next, the basic characteristics of coupled vibration control structures connected using steel dampers are studied by conducting a series of analyses changing both the combination of buildings and the characteristics of the dampers. Each building model used in this paper is of a one-mass system and translation mode vibration.

[1]Research Assoc., Tokyo Metropolitan Univ., Tokyo, Japan, Email: minami-susumu@c.metro-u.ac.jp
[2]Prof., Tokyo Metropolitan Univ., Tokyo, Japan, Email: yamazaki@arch.metro-u.ac.jp
[3]Mori Building Co. Ltd, Tokyo, Japan
[4]Graduate Student, Tokyo Metropolitan Univ., Tokyo, Japan, Email: ken_thra@mac.com

TEST METHOD

Vibration Model

One-way shaking table tests are carried out for coupled vibration control structure models made by connecting two buildings with a one-mass system using steel dampers. The direction of the excitation coincides with the straight line connecting the centers of gravity of the masses of the two buildings. The dampers are arranged on this line. (See Fig.1)

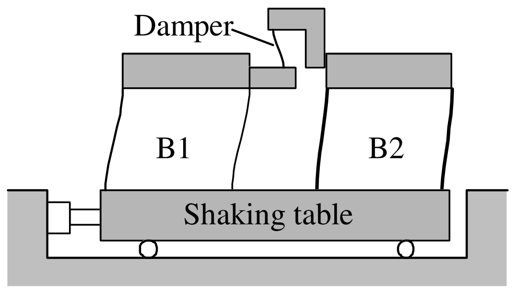

Fig.1 Vibration model

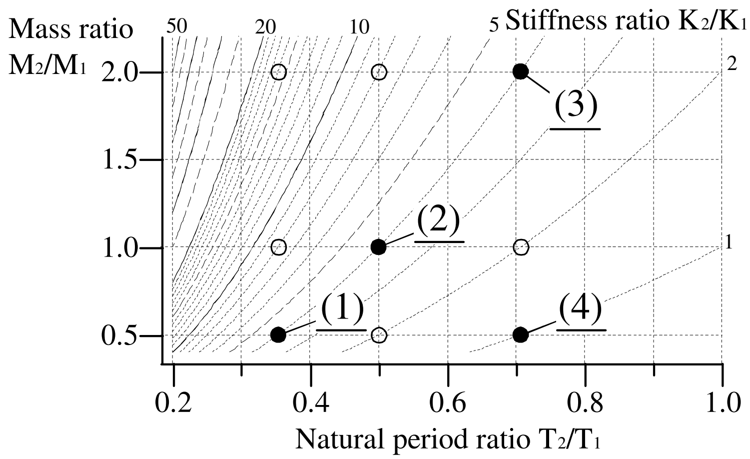

Fig.2 Combination of buildings

a. Buildings

A building with a long period is designated as B1 and a building with a short period is designated as B2. M_1, M_2, K_1, K_2 and T_1, T_2 denote the values of the mass, stiffness and natural period for B1 and B2 respectively.

Tests are carried out in the cases of four different combinations shown with ● in Fig.2 for the range of 0.35~0.7 for T_2/T_1 and 0.5~2 for M_2/M_1. Each of the combinations is referred to as (1)~(4) as shown in the figure. In the analytical investigation which will be described later, the combinations shown with ○ in the figure will be subjected to the studies.

The small-sized specimen used in this study is assumed as a 1/9 scale model and the test time is set at 1/3 of the real time by applying the model similarity law. Namely, the seismic wave input to the shaking table is reduced by 1/3 of the real wave for the time axis. The natural periods for B1 and B2 are set at 0.14~0.4sec for the modeling specimens which can be converted into 0.42~1.2sec for the real time.

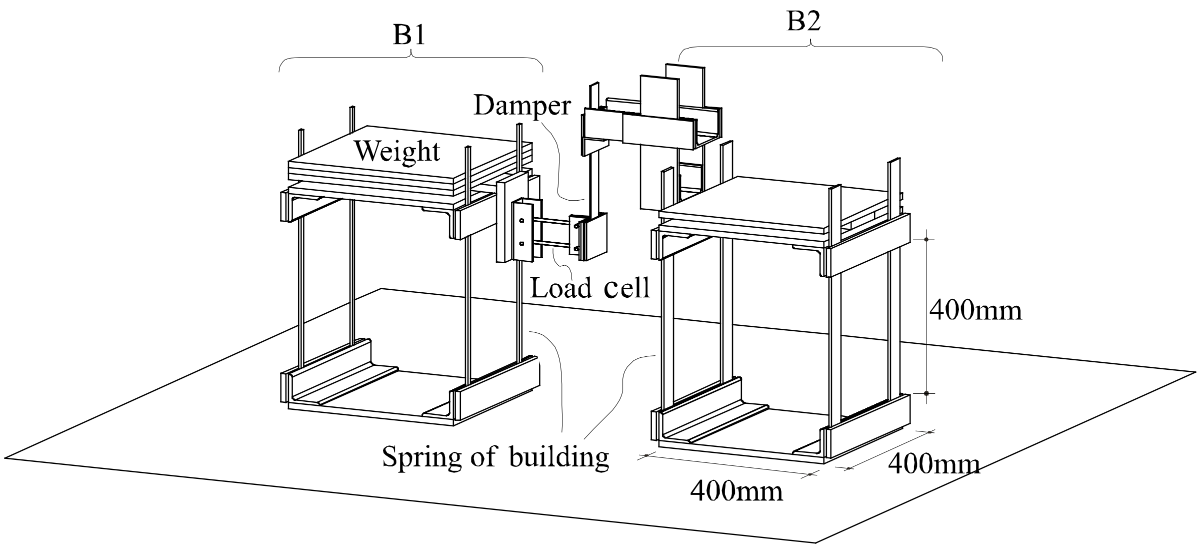

Fig.3 Test model

Fig.3 shows the shape of the model. Steel plates of SS400 are used as building springs. Table 1 shows the specifications of the vibration model for each combination of buildings. Tests are carried out mainly for the buildings in an elastic region.

Table 1 Specifications of vibration model

Combination of buildings	(1)		(2)		(3)		(4)	
	B1	B2	B1	B2	B1	B2	B1	B2
Natural period [s]	0.40	0.14	0.40	0.20	0.28	0.20	0.20	0.14
T_2/T_1	0.35		0.5		0.7		0.7	
Mass [kg]	120	60	120	120	60	120	120	60
M_2/M_1	0.5		1		2		0.5	
Stiffness [N/cm]	290	1150	290	1150	290	1150	1150	1150
K_2/K_1	4		4		4		1	

b. Dampers

The energy absorption of the damper is caused by the bending yield of beams. Fig.3 shows the condition of the dampers fitted to the buildings. Three different types of damper (a), (b) and (c) are used for each combination of buildings as shown in Table 2. The dampers are made of SS400 steel plates with the sickness of 3.2mm. The shape of the damper was decided based on the results of preliminary analysis. The value for the stiffness (calculated) indicated in Table 2 is obtained assuming that the rotation of both ends of the damper is fixed. The value for the stiffness (revised) is obtained by multiplying the above value by 0.65. The correction coefficient of 0.65 is used due to the fact that the ratio of the real elastic stiffness of the damper to the calculated stiffness is estimated to be 0.65 from the loading test for dampers.

Table 2 Specifications of dampers

	(a)	(b)	(c)
Width × Thickness × Length [mm]	4×3.2×80	12×3.2×10	24×3.2×11
Stiffness (calculated) [N/cm]	527	809	1216
Stiffness (revised) [N/cm]	343	524	790
Yield strength [N]	72	172	313

c. Input seismic wave

El Centro 1940 NS components (hereafter referred to as El Centro) and JMA-Kobe 1995 NS components (hereafter referred to as Kobe) are used as the input seismic wave. Each input wave is scaled by multiplying a constant value so that the maximum acceleration can be the target value. The displacement response spectra in the case of the maximum acceleration being 100cm/s^2 and the damping factor being 0.003 are shown in Fig.4.

Test conditions are summarized in Table 3.

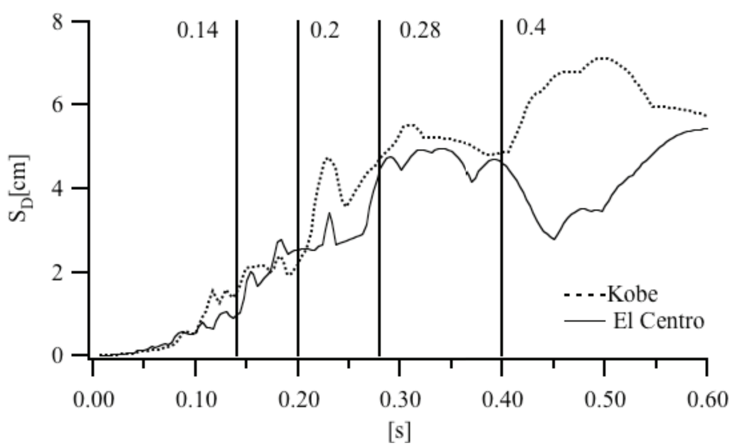

Fig.4 Displacement response spectra

Table 3 Test conditions

Combination of buildings	Damper	Seismic wave	Maximum acceleration
(1)	(a)		100 cm/s^2
(2)	(b)	El Centro	300 cm/s^2
(3)	(c)	Kobe	500 cm/s^2
(4)	Non-coupled		1000 cm/s^2

TEST RESULTS

Loading Tests for Dampers

Fig.5 shows the details of the damper.

Fig.6 shows the results of the coupon tests for the steel plate used for the damper.

In order to investigate the static and dynamic characteristics of the damper, loading tests were carried out for the damper. The setting up conditions for the loading tests are shown in Fig.7 a). A high speed hydro servo actuator was used. The loading speed was set at static loading, 20cm/s and 40cm/s. The loading speed of 20cm/s and 40cm/s correspond nearly to the maximum speed of the damper in the case of 300cm/s^2 and 1000cm/s^2 wave being input for the shaking table tests. The loading pattern was two times cyclic loading with constant amplitude. The size of the steel plate for the damper is width×thickness×length=8×3.2×80mm, which is between the sizes of damper (a) and damper (b) (See Table 2) used in the shaking table tests.

Fig.7b) and Fig.7c) show the loading speed history and the relationship between the load (F_d) and the displacement (δ_d) of the damper obtained from the tests.

The value for the elastic stiffness obtained from the tests was 65% of the stiffness value calculated under the assumption of both ends being fixed. It is discernible that the yielding load tends to increase with the rise in the loading speed. As a whole, the loading speed has little effect upon the inelastic behavior of the damper.

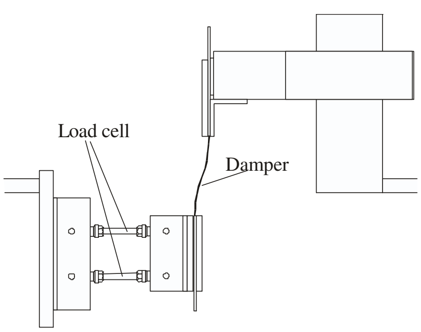

Fig.5 Details of damper

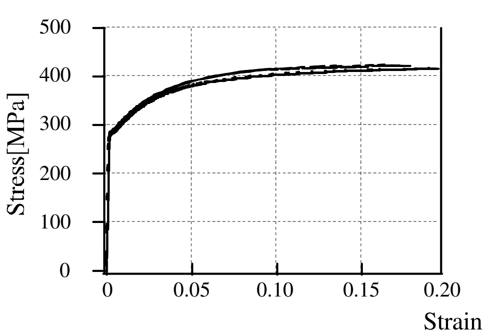

Fig.6 Strain strength relation of damper steel

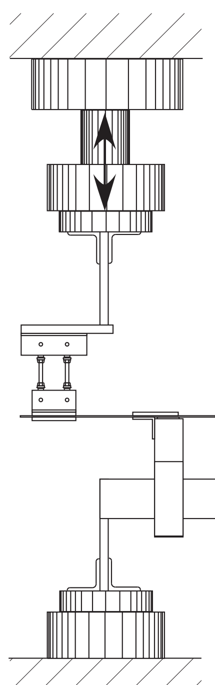

a) Test setup

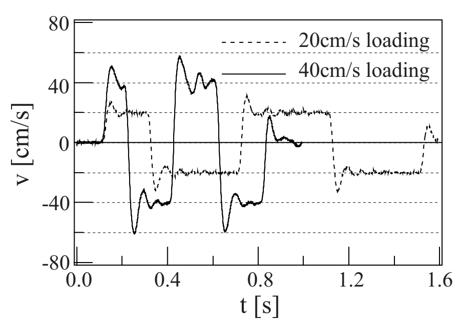

b) Loading speed

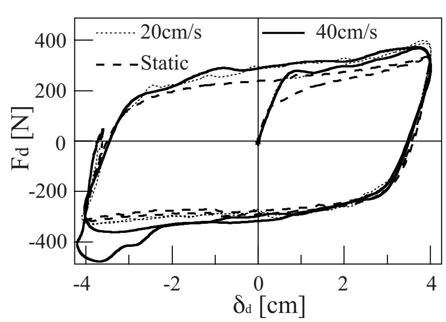

c) Load-deflection relation

Fig.7 Loading test for damper

Free Vibration Tests
For the purpose of investigating the natural period and the damping factor of the building model, free vibration tests were carried out on a non-coupled model.

Fig.8 shows the relationship between the peak-to-peak amplitude and the damping factor. It is made clear that the damping factor is about 0.2~0.7% and that it depends on the amplitude. A difference was discernible between the amplitude and the damping factor for each of two kinds of springs (stiffness 1150N/cm, 290N/cm) used in the building.

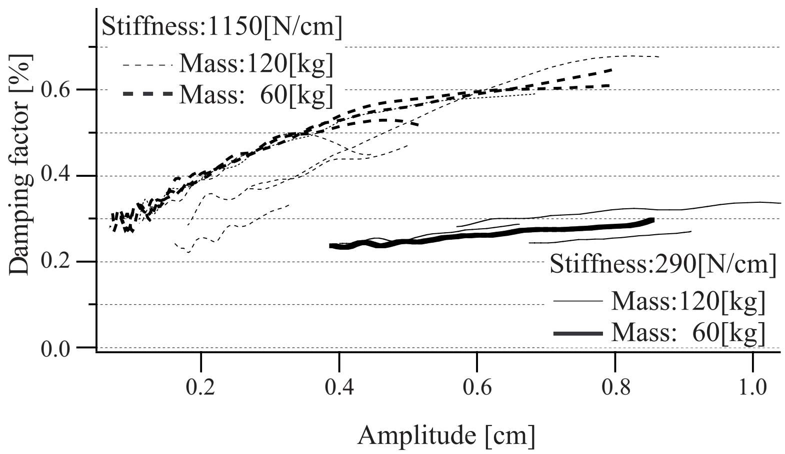

Fig.8 Relationship between amplitude and damping factor

Shaking Table Tests
Time History Displacement and Load Displacement Relations
Examples of the test results are shown in Figs.9 and 10. Fig.9 shows the results obtained in the case of the combination of building (2), damper (a) and El Centro of 100cm/s^2. Fig.10 shows the results in the case of the combination of building (2), damper (c) and El Centro of 1000cm/s^2. In each of the figures, left figures, middle figures and right figures show the test results for the non-coupled model, the test results for the coupled model and the analytical results for the coupled model obtained using the method which will be described later, respectively. In the figure for the load displacement relations of B1 and B2, the yield displacement (2.1cm) of the building spring is indicated using a broken line.

It can be seen in Fig.9 that although the ground motion acceleration is small and the plastic deformation of the damper is comparatively slight, the response of both coupled buildings decrease compared with the non-coupled case. In particular, the maximum displacement of B1 falls by 66% and the response occurring 2sec after the beginning of the vibration greatly decreases.

It is made clear from Fig.10 that both buildings are in a plastic state for the non-coupled model, but that in the coupled condition B2 shows an elastic response. With regard to B1, the absorbed plastic energy decreases and no residual displacement occurs in the coupled model.

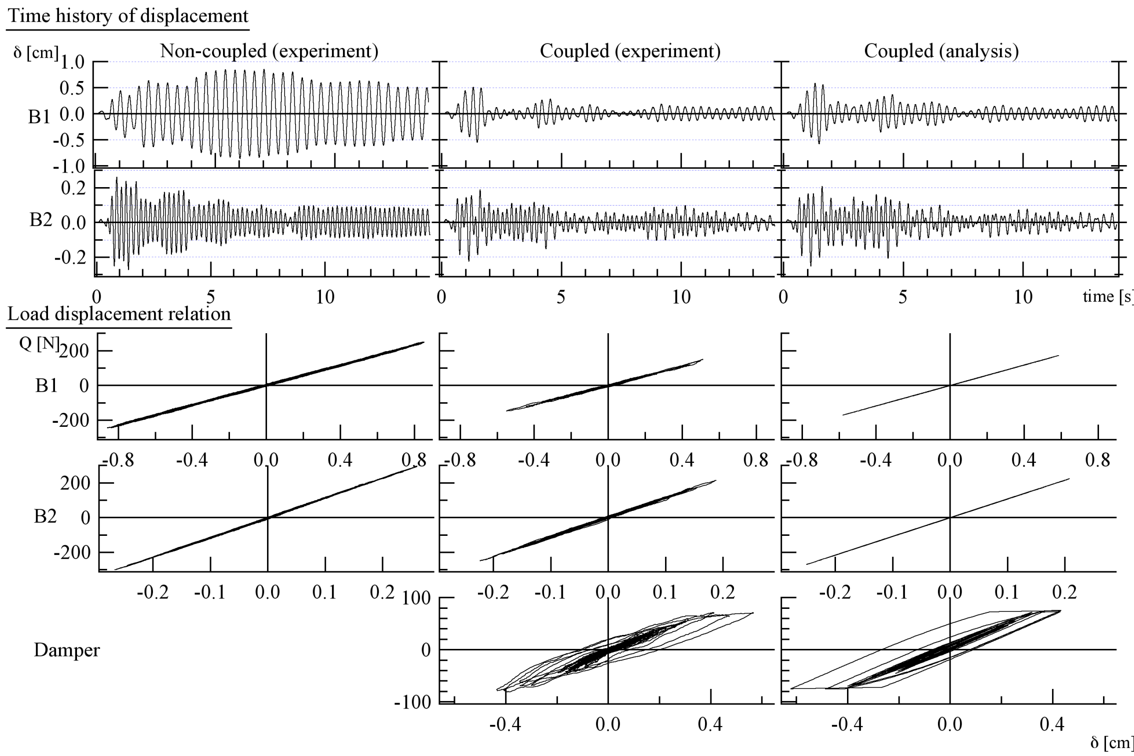

Fig.9 Test results: combination of building (1), damper (a), El Centro 100cm/s^2

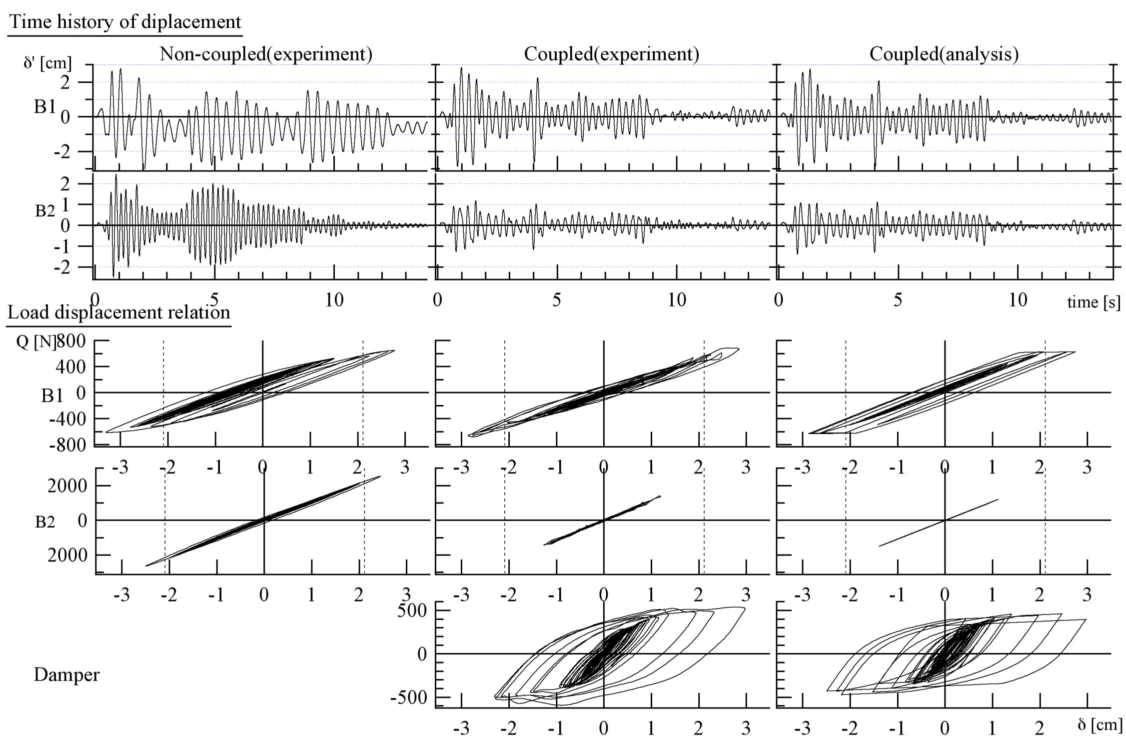

Fig.10 Test results: combination of building (1), damper (c), El Centro 1000cm/s^2

Vibration Control Effects

In this paper, the maximum displacement ratio of d obtained in the following equation is set as an index with regard to the vibration control effects.

$$d = \frac{D_{\max}}{D_{\max 0}}$$

where $D_{\max}$: Maximum displacement in the case of a coupled condition,
$D_{\max 0}$: Maximum displacement in the case of a non-coupled condition

The characteristics of the histeresis damper can be indicated mainly by the yield strength and the elastic stiffness. The non-dimensional indexes corresponding to these are set as α and β obtained from the following equation.

$$\alpha = \frac{Q_p}{M_1 \cdot \ddot{x}_{0\max}} \quad , \qquad \beta = \frac{K_e}{K_1}$$

Where Q_p: Yielding force, K_e: Elastic stiffness of damper
M_1: Mass of B1, K_1: Elastic horizontal stiffness of B1
$\ddot{x}_{0\max}$: Maximum acceleration of input wave

The Table 4 shows the region of α for the combination of buildings (1)~(4) and the value of β.

Table 4 α, β in experiments

		(1)	(2)	(3)	(4)
α	Max	2.61	2.61	5.22	2.61
	Min	0.66	0.66	0.12	0.06
β	(a)	1.18	1.18	1.18	0.30
	(b)	1.81	1.81	1.81	0.45
	(c)	2.72	2.72	2.72	0.69

The relationship between α and d for each combination of buildings is shown in Fig.11. The upper part of the figure shows the relationship in the case of El Centro being input and the lower part shows that in the case of Kobe. ○ and △ indicate the maximum displacement ratio for B1. ● and ▲ indicate the displacement for B2. △ and ▲ indicate the relationship in the case of the buildings being in a plastic state.

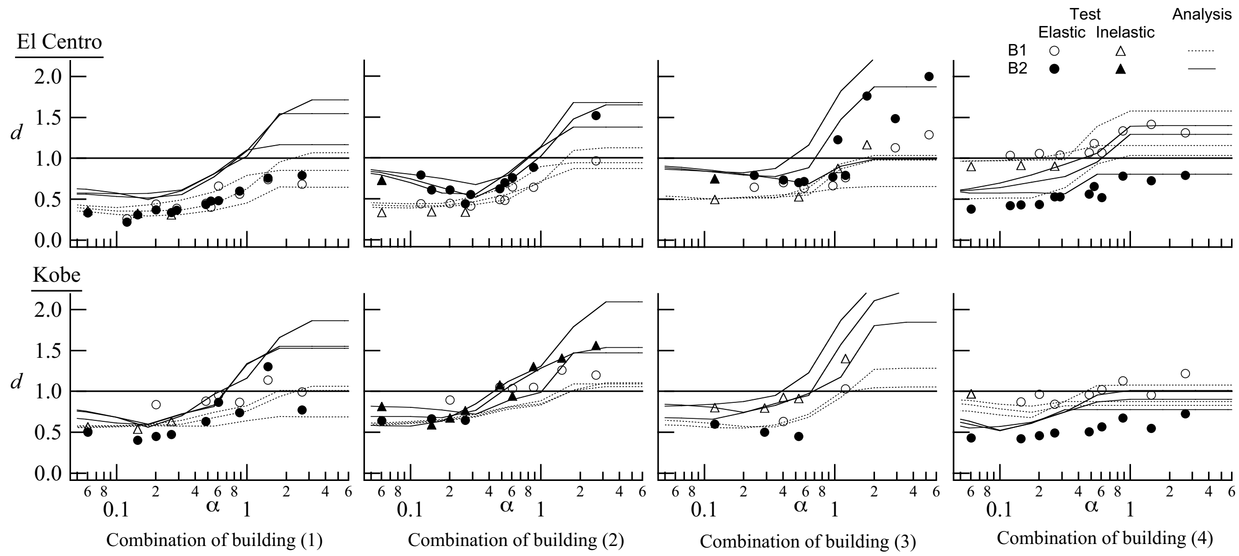

Fig. 11 α-d relation

Analysis method [3]

a. Building model

The value for the mass of the building model is set to be equal to that of the test specimen. The elastic stiffness is established so that the natural period can agree with the period obtained from the free vibration tests. The skeleton curve for the restoring force characteristics of the spring is set to be of a bi-linear type. The stiffness after yielding is set at 3% of the elastic stiffness. The damping factor is set at 0.003.

b. Damper model

The elastic stiffness is established at 65% of the stiffness obtained assuming that both ends of the damper are fixed. The damping factor is set at 0.

Time History Displacement and Load Displacement Relations

It is made clear from Figs.9 and 10 that the test results and the analysis results correspond quite well to each other.

Vibration Control Effects

Three kinds of dampers are used for each building combination. The relationship between α and d obtained from the analyses carried out varying the amount of the input ground motion for each damper is shown in Fig.11 using a dotted line and a solid line. It is discernible that the analysis results correspond well to the vibration control characteristics obtained from the tests.

INVESTIGATION BY ANALYSES

Subjects of Analyses

a. Combination of buildings

In addition to the four combinations of buildings shown in Fig.2 with marks ●, five more combinations shown with ○ are the subjects of the analyses. These nine combinations satisfy the condition of $0.35 \leq T_2/T_1 \leq 0.7$ and $0.5 \leq M_2/M_1 \leq 2.0$. The springs of the building are in an elastic state.

b. Damper characteristics

In order to obtain the maximum displacement ratio of *d*, response analyses are carried out for $13\times13=169$ cases by varying α and β into 13 steps at equal intervals on the logarithmic axis for each from 0.01 to 10 for α and from 0.1 to 5 for β.

c. Input ground motion

El Centro and Kobe waves are used as the input ground motions.

Damper Characteristics and Maximum Displacement Ratio

As for one combination of buildings and the input seismic wave, contour-lines of *d* can be drawn based on the value obtained at 169 points on the plane of α–β. Figs.12 and 13 illustrate examples of these contour-lines. These contour-lines are drawn for the combination of buildings of (2). Fig.12 shows an example in the case of El Centro and Fig.13 shows an example in the case of Kobe. The upper part in the figure shows the maximum displacement ratio of *d* for B1 and the middle part shows *d* for B2. The lower part illustrates the contour-line for the sum of the values of *d* for B1 and B2. From these figures, the following can be clarified.

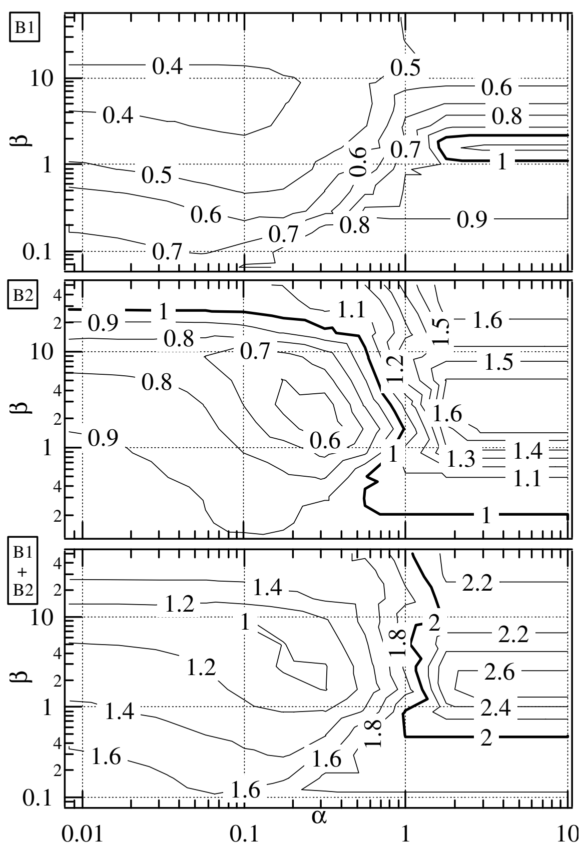

Fig.12 Contour lines of *d* : combination of building(2), El Centro wave

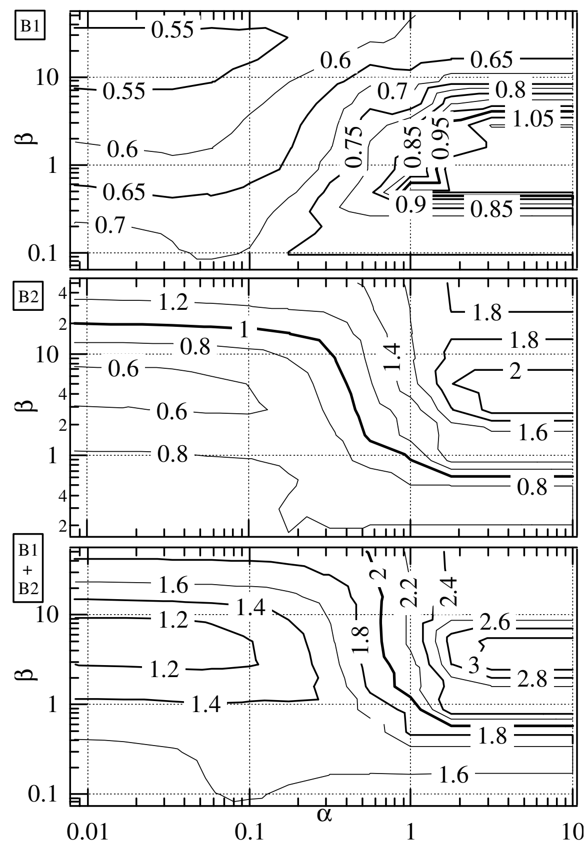

Fig.13 Contour lines of *d* : combination of building (2), Kobe wave

1) With the change in the seismic wave, the contour-line varies, but the overall tendencies for the contour-lines in Fig.12 and 13 are similar to each other.
2) The combination of α and β which makes the minimum value of *d* is the optimum condition. The optimum condition differs depending upon the *d* value for each building and the total *d* value. In

Figs.12 and 13, *d* shows the values close to the optimum for about $0.01 \leq \alpha \leq 0.3$ and $2 \leq \beta \leq 5$. Namely, regardless of the seismic wave, there are regions for α and β which can be thought to be optimum for B1 and B2.

3) It can be thought that there is a minimum limit value for α determined by the steel characteristics or the shape of the damper. Clarifying the limit value for α is a problem to be solved in the future. It can also be judged that since the minimum value for α in the shaking table tests is 0.06, under the assumption of 0.06 being the limit value for α on the conservative side, the nearly optimum vibration control effects can be obtained in the range of $0.06 \leq \alpha \leq 0.3$, that is to say from the case of the maximum input amount to the case of the input amount of 1/5 of the maximum.

Furthermore, as for the other combinations of buildings, the same tendencies as those shown in Figs.12 and 13 can be seen.

Combination of Buildings and Maximum Displacement Ratio

The maximum displacement ratio for α and β in the vicinity of the optimum vibration control conditions for each combination of buildings is compared. In Fig.14, twenty values taken out in order from the minimum value of *d* among those at 169 points obtained from the analyses are plotted as the values on the ordinate. From these figures, the following can be said as a general tendency.

1) The vibration control effects in the case of El Centro being input are greater than those in the case of Kobe.
2) The vibration control effects on B1 with a long period are greater.
3) In the case of the same mass ratio, the smaller the period ratio, the greater the vibration control effects.
4) In the case of the same period ratio, no clear tendency can be seen for the influence of the mass ratio upon the vibration control effects.

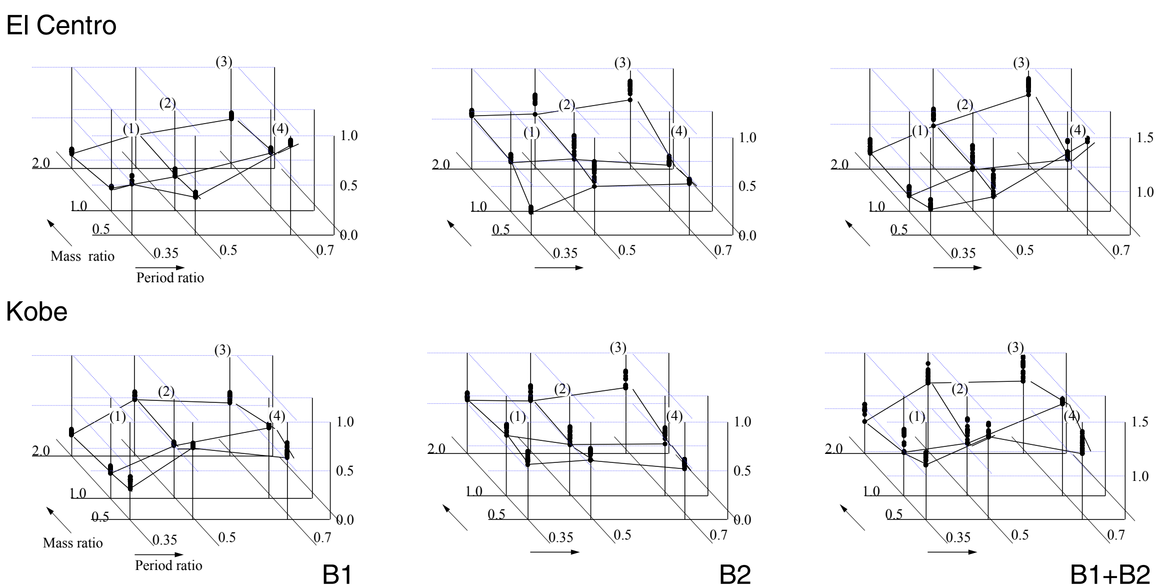

Fig.14 Relationship between mass ratio, period ratio and maximum displacement ratio

CONCLUSIONS

Vibration control effects of a coupled vibration control structure made by connecting one-mass building models using hysteresis dampers were studied carrying out shaking table tests and response analyses.

In this paper, the range for the period ratio of two buildings subjected to the study was set at 0.35~0.7 and the range for the mass ratio was 0.5~2.0. El Centro (NS) and JMA-Kobe (NS) were used as the input wave. The vibration control effects were evaluated using the maximum displacement ratio (ratio of the maximum displacement in the case of a coupled condition to the maximum displacement in the case of a non-coupled condition).

The results obtained from this study can be summarized as follows:

1) The smaller the period ratio, the greater the vibration control effects.
2) There are regions of the stiffness and yield strength of a damper in which optimum vibration control effects can be obtained for each combination of buildings.
3) If using an appropriate damper, almost optimum vibration control effects can be obtained in the range from the maximum input amount to 1/5 of this amount.

REFERENCES

1. Kobori, T., “Response control structure”, Kajima Press, 1993.
2. Kageyama, M., Yasui, Y. and Seto, K., “The principal solutions of connecting spring and damper for optimum vibration control under several criteria”, Journal of Structural and Construction Engineering (Transactions of AIJ), 2000; No.529: 97-104.
3. Yamazaki, S., Minami, S., Mimura, H. and Udagawa, K., “Effect of vertical ground motions on earthquake response of steel frames”, 12WCEE, 2000.